

# Renormalization group flow of SU(3) lattice gauge theory - Numerical studies in a two coupling space -

QCDTARO Collaboration

## Abstract

We investigate the renormalization group flow of SU(3) lattice gauge theory in two coupling space with  $\beta_{11}$  of plaquette and  $\beta_{12}$  of rectangular actions. Extensive numerical calculations of the RG flow are made in the fourth quadrant of the coupling space, i.e.,  $\beta_{11} > 0$  and  $\beta_{12} < 0$ . Swendsen's factor 2 blocking and Schwinger-Dyson method are used to find an effective action for the blocked gauge field. Resultant renormalization group flow runs quickly towards an attractive stream which has approximate line shape. This is a numerical evidence of the renormalized trajectory which locates close to the two coupling space. A model flow equation which incorporates a marginal coupling (asymptotic scaling term), an irrelevant coupling and a nonperturbative attraction toward strong coupling limit reproduces qualitatively the observed feature. We further examine scaling property of an action which is closer to the attractive stream than the currently used improved actions. It is found that the action shows excellent restoration of rotational symmetry even for coarse lattices with  $a \sim 0.4$  fm.

## 1 Introduction

Since Wilson's first numerical renormalization group (RG) analysis of SU(2) gauge theory [1], there have been many Monte Carlo RG studies of non-perturbative  $\beta$ -functions (see Ref.[2] and references therein). In these analysis indirect informations about the  $\beta$  function, such as  $\Delta\beta$ , have been obtained [3]. Recent progress of lattice techniques [4, 5, 6] allows us to estimate directly the RG flow in a multi-coupling space[7].

We study renormalization effect by blocking transformation which changes lattice cut-off but leaves long range contents invariant. New blocked actions  $S'$  as a function of blocked link variables  $V$ 's are constructed from the original  $S(U)$  as

$$e^{-S'(V)} = \int e^{-S(U)} \delta(V - P(U)) DU, \quad (1)$$

where  $P$  defines the blocking transformation. The action  $S'$  includes the renormalization effect induced by blocking. In the space of coupling constants, the blocking transformation makes a transition from a point corresponding to  $S$  to a new one of  $S'$ . Repeating the blocking transformation, we obtain trajectories in the coupling space called as the renormalization group flow.

There is a special trajectory, i.e., renormalized trajectory (RT) which starts at the ultra-violet fixed point. On RT, actions keeps long range contents corresponding to continuum physics. Recently Hasenfratz and Niedermayer have reminded us the point and called the action on the RT as a "perfect action" [9]. Therefore if we find a RT corresponding to a blocking transformation, it gives us an action which gives accurate results in the continuum limit. Even if it is an approximate one, it serves a well-improved action. In this sense, a

pioneering work has been done by Iwasaki more than ten years ago [8]. He estimated a RT by matching Wilson loops (based on a perturbative approximation), and proposed an improved action.

In this work, we make a numerical analysis of the RG flow in two coupling space,  $(\beta_{11}, \beta_{12})$  of SU(3) lattice gauge theory, and clarify structure of the renormalization group flow. Namely, the action is restricted in the following form;

$$S = \beta_{11} \sum_{plaq} \left(1 - \frac{1}{3} \text{ReTr} P_{plaq}\right) + \beta_{12} \sum_{rect} \left(1 - \frac{1}{3} \text{ReTr} P_{rect}\right) \quad (2)$$

Here  $P_{plaq}$  and  $P_{rect}$  correspond to  $1 \times 1$  and  $1 \times 2$  loops, respectively.

Main purpose of the present work is to perform extensive study beyond perturbative analysis. It is not trivial that the RT locates near two coupling space. If no remnant of the RT can be seen, the two coupling space is insufficient to obtain well improved actions. In this sense, global analysis from weak to strong coupling regions of the RG flow is indispensable.

Analysis is made in the fourth quadrant of the coupling space. We examine renormalization effects induced by Swendsen's factor two blocking for the plaquette action and some improved actions. In addition, wider analysis is made to clarify the global structure of the RG flow. We will find a structure which attracts the flows. This is an evidence that the RT sits close to the coupling space. Characteristic features in the strong and weak coupling regions are also found. Observed features are reproduced by a model flow equation which incorporates a marginal coupling (asymptotic scaling term), an irrelevant coupling and a nonperturbative attraction toward strong coupling limit.

Based on the flow structure, we further examine scaling property of an action in the two coupling space. Tests are made for rotational invariance and scaling of  $\sqrt{\sigma}/T_c$ . Near the attractive stream, we find good restoration of rotational invariance.

This paper is organized as follows. In section 2, basic tools for the analysis are given. Section 3 is devoted to state simulation and numerical results of the RG flow. Scaling test of the actions is described in section 4. In section 5, a model flow equation which can reproduce the RG flow is proposed. Summary and discussions are given in section 7.

## 2 Blocking transformation and determination of renormalization effects

Here we describe basic frame work to study the RG flow for SU(3) gauge field on the lattice. First we produce field configurations with an action  $S$  which has coupling constants  $(\beta_{11}, \beta_{12}, \dots)$ , and apply a blocking transformation on these configurations. Next we determine an action  $S'$  with coupling constants  $(\beta'_{11}, \beta'_{12}, \dots)$  which reproduces the transformed configurations. Then we get the flow from original coupling constants  $\{\beta\}$  to transformed ones  $\{\beta'\}$  in the coupling constant space; this is the RG flow.

In order to perform the blocking transformation on a lattice, we adopt Swendsen's factor-two blocking [11]. For a set of SU(3) link variables  $U_\mu(n)$ , a blocked field is constructed as:

$$Q_\mu(n) = U_\mu(n)U_\mu(n + \hat{\mu}) + c \sum_{\nu \neq \mu} U_\nu(n)U_\mu(n + \hat{\nu})U_\mu(n + \hat{\nu} + \hat{\mu})U_\nu^\dagger(n + 2\hat{\mu}). \quad (3)$$

Here  $c$  is a parameter to control weight of staple-like path. Projection of  $Q_\mu(n)$  to blocked SU(3) gauge field  $V_\mu(n)$  is made by maximizing  $\text{ReTr}(Q_\mu(n)V_\mu^\dagger(n))$ .

To determine the effective action  $S'$  on blocked configuration  $V$ , we use Schwinger-Dyson method [4]. This is based on the following identity. For a link  $V_l$ , consider quantities;

$$\langle \text{ImTr}(\lambda^c V_l G_l^\alpha) \rangle = \frac{1}{Z} \int \mathcal{D}V \text{Im Tr}(\lambda^c V_l G_l^\alpha) e^{-S'} \quad (4)$$

where  $\lambda^c$  stands for Gell-Mann matrices.  $G_l$  is a sum of "staples"  $G_l^\gamma$  for the link  $l$ ,  $G_l = \sum_\gamma (\beta_\gamma/6) G_l^\gamma$ . The action  $S'$  is assumed to have the form  $\sum_l \text{Re Tr} V_l G_l$ . For the present analysis,  $\gamma$  corresponds to a plaquette and a rectangle. Eq.(4) should be invariant under the change of variable  $V_l \rightarrow (1 + i\epsilon\lambda^c)V_l$ . Setting terms linear in  $\epsilon$  to be zero, we get the identity,

$$\int \mathcal{D}V [\text{ReTr}((\lambda^c)^2 V_l G_l^\alpha) + \text{ImTr}(\lambda^c V_l G_l^\alpha) \text{ImTr}(\lambda^c V_l G_l)] e^{-S'} = 0. \quad (5)$$

Summing the formula over  $c$  (5), we obtain Schwinger-Dyson equation,

$$\begin{aligned} \frac{8}{3} \text{Re} \langle \text{Tr}(V_l G_l^\alpha) \rangle &= \sum_\gamma \frac{\beta_\gamma}{6} \{ -\text{Re} \langle \text{Tr}(V_l G_l^\alpha V_l G_l^\gamma) \rangle \\ &+ \text{Re} \langle \text{Tr}(G_l^\alpha (G_l^\gamma)^\dagger) \rangle - \frac{2}{3} \langle \text{Im Tr}(V_l G_l^\alpha) \text{Im Tr}(V_l G_l^\gamma) \rangle \}. \end{aligned} \quad (6)$$

Here we used an identity:  $\sum_{c=1}^8 \text{Tr}(\lambda^c A) \text{Tr}(\lambda^c B) = 2\text{Tr}AB - \frac{2}{3}\text{Tr}A\text{Tr}B$ . We apply this equation to the blocked configurations, and calculate the expectation values  $\langle \dots \rangle$  on both sides. Now Eq.(6) may be considered as a set of linear equations with  $\beta_\gamma$ 's as unknowns. It is noted that we may use other loop operators instead of  $G^\alpha$ . However a minimal choice is to take the same  $G^\alpha$ 's with ones in the action. In this case, the number of equations is equal to the number of unknowns in the coupling space.

Another remark is that canonical Demon method also works for the present purpose.[6] It tunes effective action so as to reproduce mean values of plaquette and rectangular loop whereas Schwinger-Dyson method respects wider loops which are combination of staples such as  $\text{Tr}(G_l^\alpha (G_l^\gamma)^\dagger)$ . In case of limited coupling space, they may give different actions. Since systematic errors of both methods are not known in the present stage, only the results by Schwinger-Dyson method are presented in this work.

Since we study the RG flow in two coupling space, we show a Schwinger-Dyson equation for two coupling space explicitly. The  $\beta^V$ 's are blocked coupling constants.

$$\begin{aligned} \langle \text{Re Tr}(P_{\mu\nu}^i) \rangle &= \frac{\beta_{11}^V}{16} \sum_{\sigma \neq \mu} [-\langle \text{Re Tr}(P_{\mu\nu}^i P_{\mu\sigma}^{(1)}) \rangle + \langle \text{Re Tr}(P_{\mu\nu}^i P_{\mu\sigma}^{(1)\dagger}) \rangle] \\ &\quad - \frac{2}{3} \langle \text{Im Tr}(P_{\mu\nu}^i) \text{Im Tr}(P_{\mu\sigma}^{(1)}) \rangle \\ &+ \frac{\beta_{12}^V}{16} \sum_{\sigma \neq \mu} [-\langle \text{Re Tr}(P_{\mu\nu}^i P_{\mu\sigma}^{(2)}) \rangle + \langle \text{Re Tr}(P_{\mu\nu}^i P_{\mu\sigma}^{(2)\dagger}) \rangle] \\ &\quad - \frac{2}{3} \langle \text{Im Tr}(P_{\mu\nu}^i) \text{Im Tr}(P_{\mu\sigma}^{(2)}) \rangle \\ &\quad - \langle \text{Re Tr}(P_{\mu\nu}^i P_{\mu\sigma}^\Gamma) \rangle + \langle \text{Re Tr}(P_{\mu\nu}^i P_{\mu\sigma}^{\Gamma\dagger}) \rangle \end{aligned}$$

$$\begin{aligned}
& -\frac{2}{3} \langle \text{Im Tr}(P_{\mu\nu}^i) \text{Im Tr}(P_{\mu\sigma}^\Gamma) \rangle \\
& - \langle \text{Re Tr}(P_{\mu\nu}^i P_{\mu\sigma}^\Delta) \rangle + \langle \text{Re Tr}(P_{\mu\nu}^i P_{\mu\sigma}^{\Delta\dagger}) \rangle \\
& - \frac{2}{3} \langle \text{Im Tr}(P_{\mu\nu}^i) \text{Im Tr}(P_{\mu\sigma}^\Delta) \rangle,
\end{aligned} \tag{7}$$

for  $i = 1, 2$ , where

$$P_{\mu\nu}^1(n) = V_\mu(n) V_\nu(n + \hat{\mu}) V_{-\mu}(n + \hat{\mu} + \hat{\nu}) V_{-\nu}(n + \hat{\nu}) \tag{8}$$

$$\begin{aligned}
P_{\mu\nu}^2(n) &= V_\mu(n) V_\nu(n + \hat{\mu}) V_\nu(n + \hat{\mu} + \hat{\nu}) \\
& V_{-\mu}(n + \hat{\mu} + 2\hat{\nu}) V_{-\nu}(n + 2\hat{\nu}) V_{-\nu}(n + \hat{\nu})
\end{aligned} \tag{9}$$

$$\begin{aligned}
P_{\mu\nu}^\Gamma(n) &= V_\mu(n) V_\nu(n + \hat{\mu}) V_{-\mu}(n + \hat{\nu}) \\
& V_{-\mu}(n - \hat{\mu} + \hat{\nu}) V_{-\nu}(n - \hat{\mu}) V_\mu(n - \hat{\nu})
\end{aligned} \tag{10}$$

$$\begin{aligned}
P_{\mu\nu}^\Delta(n) &= V_\mu(n) V_\mu(n + \hat{\mu}) V_\nu(n + 2\hat{\mu}) \\
& V_{-\mu}(n + 2\hat{\mu} + \hat{\nu}) V_{-\mu}(n + \hat{\mu} + \hat{\nu}) V_\nu(n + \hat{\nu})
\end{aligned} \tag{11}$$

and we use convenient notation,  $V_{-\mu}(n) = V_\mu^\dagger(n - \hat{\mu})$ . Wilson loops,  $P_{\mu\nu}$ 's, are evaluated on the blocked configurations and Schwinger-Dyson equation is numerically solved.

### 3 Simulation and numerical results of RG flow

Utilizing the techniques in the previous section, coupling flow by factor 2 blocking is studied. We set the blocking parameter  $c = 0.5$ .

Series of simulations on lattices of size  $8^4$  and  $16^4$  are performed. Finite temperature phase transition of those lattice in the case of Wilson action is approximately  $\beta_{11} = 5.9$  and  $6.3$  which roughly correspond to  $a\sqrt{\sigma} = 0.27$  and  $a\sqrt{\sigma} = 0.14$  respectively. Therefore, those lattices enable us to study flow analysis in the confinement phase up to those lattice spacing. Studies in the deconfinement phase are also carried out in the present work. This is possible since the blocking does not affect long range dynamics and it is irrespective of the phase. We check this point by comparing results whose phases are confined on  $16^4$  lattice while deconfined on  $8^4$  lattice. The results agree within errors.

Surveyed region in the present work is the fourth quadrant which covers improved actions presently known. Blockings are carried out at more than 30 points. At each point about 100 configurations separated by every 100 sweeps are used to determine renormalized couplings  $\beta_{11}$  and  $\beta_{12}$  by Schwinger-Dyson method. Pseudo heatbath method is used to generate the gauge fields. Typical errors in the determination of the coupling are shown in Table 1. The errors are relatively small even at deconfined points. In order to check auto correlation, analyses are made for data sample in which each configuration is separated by 1000 sweeps. Those data agree with that of the standard samples within error bars.

Results are summarized in Fig 1, in which the resultant coupling shift by the blocking is shown by arrows.

| $\beta_{11}$ | $\beta_{12}$ | $\beta_{11}^V$ | $\beta_{12}^V$ |
|--------------|--------------|----------------|----------------|
| 7.00         | 0.0          | 13.188(22)     | -1.6564(94)    |
| 7.00         | -0.35        | 8.148(29)      | -1.0431(98)    |
| 11.00        | -0.9981      | 15.189(73)     | -2.329(19)     |
| 13.20        | -1.493       | 15.445(50)     | -2.559(15)     |
| (†)13.20     | -1.493       | 15.519(37)     | -2.583(13)     |

Table 1. Typical errors of  $\beta_{11}^Y$  and  $\beta_{12}^Y$  by Schwinger-Dyson method. A hundred configurations are used at each point. For the data ( $\dagger$ ), measurements are done at every 1000 pseudo heatbath step.

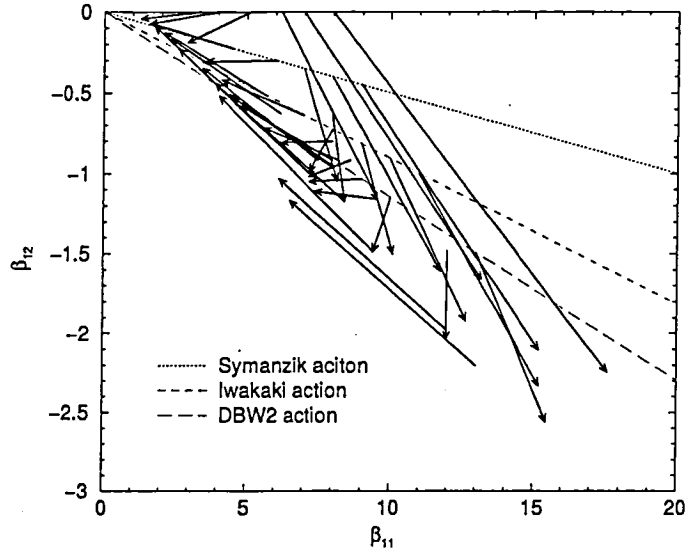


Figure 1: Renormalization group flow for QCD in two coupling space. The line in which these arrows involve is the renormalized trajectory.

As shown in the figure, several characteristics of the flow are seen. If we start from plaquette action ( $\beta_{12} = 0$  line), renormalization results in negative  $\beta_{12}$  as expected by perturbative analysis. At  $\beta_{11} = 6 \sim 8$ , renormalization is very strong and make  $\beta_{11}$  twice larger and  $\beta_{12}$  negative. Resultant points are far below the line of tree Symanzik action. On the other hand, in the strong coupling region below  $\beta_{11} < 5$ , the  $\beta_{11}$  is reduced by the renormalization. Therefore, the plaquette action suffers large renormalization and it is far from the renormalization trajectory.

Points on the tree Symanzik action,  $\beta_{12}/\beta_{11} = -0.05$ , are RG transformed onto those with  $\beta_{12}$  more negative. Although renormalization effects are reduced, trend is the same as that of the plaquette action. This means that tree Symanzik action is still far from blocking invariant. Perturbative  $O(a^2)$  improvement is insufficient at least for currently used range of lattice spacing.

Now we watch flows starting from Iwasaki action,  $\beta_{12}/\beta_{11} = -0.09073$ . We see that renormalization occurs approximately along the line up to an intermediate point ( $\beta_{11} + 8\beta_{12} \approx 2$ ). Above the point, however, flows leave from the line. Thus the present blocking transformation renormalizes Iwasaki action further and induces more negative value of  $\beta_{12}$  above intermediate coupling region.

Let us turn to the global structure of the flow. Blockings are made at the points of which  $\beta_{12}/\beta_{11} = -0.1 \sim -0.15$ . For those points, renormalization effect is relatively small and converges to a narrow stream. This is manifest at strong coupling region. As a whole, there is an attractive stream to which flows approach quickly. Furthermore, once flow reaches the stream, it runs along the stream. Therefore actions on the attractive stream are approximately blocking invariant apart from a normalization. Shape of the attractive stream is clearly identified as a parabolic curve in the strong coupling region while at points far from the

origin, it is less obvious in the present data. This is remarkable indication that renormalized trajectory locates close to the present coupling space. This is an encouraging result for finding good improved action in this two coupling space.

A close watching of the attractive flow tells more characteristics. If we start from Wilson action at  $\beta_1 > 6.0$ , the first blocking leads to larger renormalization as  $\beta_{11}$  increases and the resultant flow vectors have the same direction. This feature seems consistent with flow induced by an irrelevant coupling. In the strong coupling region, we observe another feature. The coupling turns into more deep in strong coupling region with a parabolic behavior. In section 5, we will try to reproduce these features by a model equation including an irrelevant coupling, asymptotic scaling term and a driving term caused from area law.

## 4 Scaling test of the actions near the attractive stream

Purpose of this section is to examine scaling property of the action near the attractive stream. As shown in Fig.1, we expect that the irrelevant coupling is considerably reduced and actions will be dominated by marginal coupling term. Here we take an action which is determined by double blocking from  $32^3 \times 4$  lattice with Wilson action; this action is called as DBW2 (doubly blocked from Wilson action in 2 coupling space) and the value of  $\beta_{12}/\beta_{11}$  is -0.1148.

There are many ways to test scaling. Among others, we will examine rotational invariance of heavy quark potential and independency of  $T_c/\sqrt{\sigma}$  on lattice spacing. The former is carried out in the following. Let us define a measure for violation of rotational symmetry as

$$\delta_V^2 = \sum_{off} \frac{[V(R) - V_{on}(R)]^2}{V(R)^2 \delta V(R)^2} / \left( \sum_{off} \frac{1}{\delta V(R)^2} \right) \quad (12)$$

where  $V(R)$  is static quark potential and  $\delta V(R)$  is its error.  $V(R)_{on}$  is a fitting function to only on-axis data.  $\sum_{off}$  means summations over off-axis data. This quantity is measured on the configurations generated by DBW2 action. For comparison, plaquette-, tree Symanzik and Iwasaki's improved actions are also examined.  $12^3 \times 24$  lattice is used for this purpose and simulations are made for lattice spacing  $a = 0.15 \sim 0.4\text{fm}$ . Results are summerized in Fig.2.

In the figure, horizontal axis is lattice spacing squared so as to see expected  $a^2$  effect. As seen in the figure, both Iwasaki's and DBW2 actions show excellent restoration of rotational symmetry even at  $a \sim 0.3\text{fm}$  while clear  $a^2$  violations are seen for plaquette and tree Symanzik actions. Furthermore, DBW2 action seems better than Iwasaki's action in this analysis.

Second check is examination of scaling of  $T_c/\sqrt{\sigma}$ . The critical temperature is defined as

$$T_c = 1/N_t a_c, \quad a_c = a(\beta_c) \quad (13)$$

where  $N_t$  is temporal lattice size. In order to obtain critical coupling  $\beta_c$ ,  $N_t = 3, 4, 6$  lattices are used and susceptibility of Polyakov loop is measured. Then,  $\beta_c$  is obtained by finite size scaling of  $12^3 \times 4$  and  $16^3 \times 4$  lattices. Resultant  $\beta_c$ s are given in Table 2.

| $N_t$ | lattice                                       | $(\beta_{11} + 8\beta_{12})_c(\infty)$ |
|-------|---|--|
| 3     | $10^3 \times 3, 12^3 \times 3, 14^3 \times 3$ | 0.75696(98)                            |
| 4     | $12^3 \times 4, 16^3 \times 4$                | 0.82430(95)                            |
| 6     | $18^3 \times 6$                               | 0.936(25)                              |

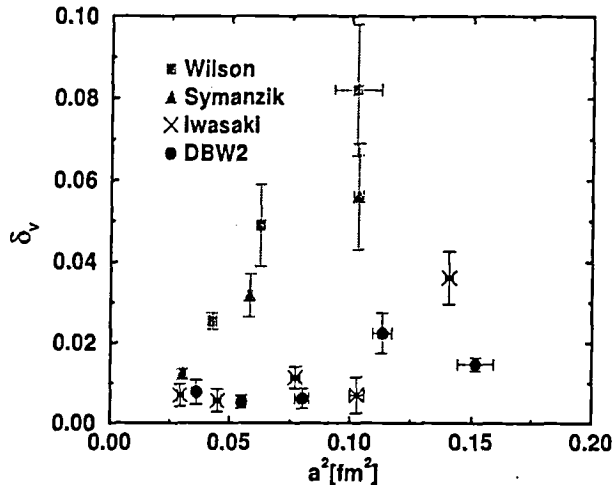


Figure 2: Rotational symmetry violation of various improved actions

Table 2. Determinations of phase transition points for the DBW2 action at finite temperature.

String tension is extracted from the static quark potential. We use Ansatz ;

$$V(R) = A + \frac{\alpha}{R} + \sigma R \quad (14)$$

| $N_t$ | $A$        | $\alpha$   | $\sigma a^2$ |
|-------|------------|------------|--------------|
| 4     | 0.550(17)  | -0.255(23) | 0.1555(28)   |
| 6     | 0.5791(96) | -0.357(22) | 0.06996(99)  |

Table 3. Determination of parameters of heavy quark potential for DBW2 action.

Determining  $\sigma$  at  $\beta_c(N_t = 3)$ ,  $\beta_c(N_t = 4)$  and  $\beta_c(N_t = 6)$  we obtain  $T_c/\sqrt{\sigma}$ . Results are

$$\begin{aligned} T_c/\sqrt{\sigma} &= 0.6340(60) \quad \text{at } N_t = 4 \\ &0.6301(65) \quad \text{at } N_t = 6 \end{aligned} \quad (15)$$

In Fig.3 we shows the results together with other data on plaquette, tree Symanzik, tad-pole improved Symanzik and Iwasaki actions from Refs [19, 20].

No appreciable dependence on lattice spacing is seen in the ration  $T_c/\sqrt{\sigma}$  for all the case including the DBW2 action. A puzzle is that the value of Iwasaki action is slightly high in comparison with other data but this may be due to technical difference to extract the string tension. Thus, DBW2 action passes this test as expected.

The results of both tests show that DBW2 action is really a well-improved as suggested by RG flow analysis.

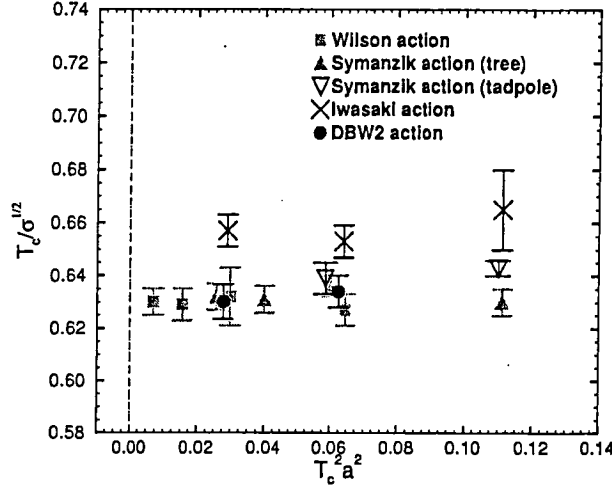


Figure 3: Scaling behavior of  $T_c/\sqrt{\sigma}$ . We compare DBW2 action with results from other actions in 2-coupling space [19, 20]

As a by-product of the  $T_c$  analysis, contours of constant lattice spacing is obtained through the relation  $a = 1/N_t T_c$ . Fig.4 shows compilation of the phase transition points in the two coupling space for plaquette, tree Symanzik, Iwasaki and DBW2 actions on  $N_t = 3 \sim 12$  lattices.

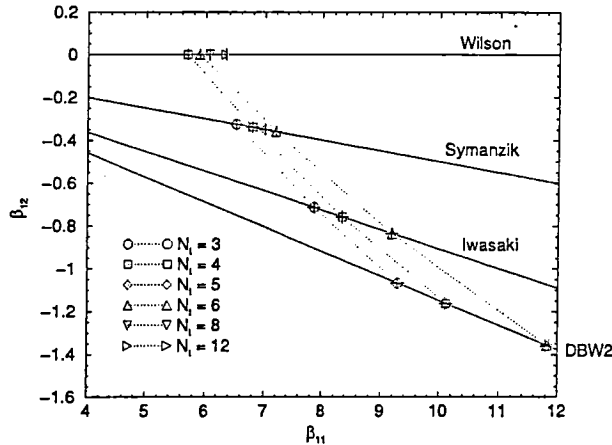


Figure 4: Symbols are the phase transition points for each  $N_t$  at thermodynamic limit. Since  $a = 1/N_t T_c$ , we can estimate  $aT_c = \text{constant}$  contours, which are indicated by dotted lines.

## 5 Modeling RG flow

In this section, we try to describe the flow in terms of a marginal and an irrelevant couplings. We have numerically obtained RG flow as in Fig.1, whose behavior is nontrivial. It is worth while to search for a mechanism of the behavior.

Let us first consider RG flow at small lattice spacing in an  $N$  dimensional coupling space.

Since our lattice is SU(3) gauge theory which has asymptotic scaling, there is a marginal (or weakly relevant) coupling. Others will be irrelevant ones which shrink with the RG transformation.

In order to describe this situation, we adopt model beta function as,

$$\frac{d\vec{\beta}}{d\ln a} = \mathbf{A}\vec{\beta} - B(\beta_n)\frac{\vec{n}}{|\vec{n}|^2} \quad (16)$$

where  $B(x)$  is perturbative beta-function

$$B(x) = 12b_0 + 72b_1/x + \dots \quad (17)$$

with  $b_0 = 33/(48\pi^2)$  and  $b_1 = (102/121)b_0^2$ .  $\mathbf{A}$  is a constant  $N \times N$  matrix which has a zero eigenvalue and its eigenvector  $\vec{w}$  and  $N - 1$  negative eigenvalues  $\lambda_i$  with eigenvector  $\vec{v}_i$  ( $i = 1, \dots, N - 1$ ).  $\vec{n}$  is a constant vector orthogonal to  $\vec{v}_i$ 's

$$(\vec{n} \cdot \vec{v}_i) = 0 \quad \text{for } i = 1, \dots, N - 1 \quad (18)$$

and  $\beta_n = (\vec{n} \cdot \vec{\beta})$ . The condition (18) assures that solution has correct asymptotic scaling behavior in a direction  $\vec{n}$ . It is noted that the vector  $\vec{w}$  is in general not orthogonal to  $\vec{v}_i$ 's.

A solution of eq.(16) is obtained as

$$\vec{\beta} = \sum_{i=1}^{N-1} (c_i a^{\lambda_i} - \frac{h_i(a)}{\lambda_i}) \vec{v}_i + \frac{\beta_p(a\Lambda)}{(\vec{n} \cdot \vec{w})} \vec{w} \quad (19)$$

where  $\beta_p(a\Lambda)$  is asymptotic scaling solution satisfying

$$\frac{d\beta_p}{d\ln a} = -B(\beta_p) \quad (20)$$

and

$$h_i = \frac{(\vec{v}_i \cdot \vec{w})}{(\vec{n} \cdot \vec{w})} a^{\lambda_i} \int_{a_0}^a du^{-\lambda_i} B(\beta_p(u\Lambda)) \quad (21)$$

Behavior of the solution (19) is easily seen.

General pattern of the flow is as follows. For simplicity, we consider  $h_i$ 's are constants. This is good approximation since  $b_0$  dominate in  $B$ . As  $a$  increases, it firstly approaches to a line,

$$\vec{\beta} = - \sum_{i=1}^{N-1} \frac{h_i(a)}{\lambda_i} \vec{v}_i + \frac{\beta_p(a\Lambda)}{(\vec{n} \cdot \vec{w})} \vec{w} \quad (22)$$

with power behavior in  $a$  and successively runs logarithmically along  $\vec{w}$ .

It is noted that asymptotic scaling is maintained for  $(\vec{n} \cdot \vec{\beta})$ ,

$$(\vec{n} \cdot \vec{\beta}) = \beta_p(a\Lambda). \quad (23)$$

In the strong coupling region, we must take into account a different ingredient. Strong coupling calculation of Wilson loop in the two coupling space gives

$$\langle W(N \times M) \rangle = (\beta_{11}/18)^{NM} + (\beta_{11}/18)^{NM-2}(\beta_{12}/18)P_1^{NM} + (\beta_{11}/18)^{NM-4}(\beta_{12}/18)^2P_2^{NM} + \dots \quad (24)$$

where  $P_k^{NM}$  is a tiling weights for filling the area by  $(NM - 2k)[1 \times 1]$  and  $k[1 \times 2]$  tiles.

We impose the area law of Wilson loops with the physical string tension  $\sigma$  as

$$\langle W(N \times M) \rangle = e^{-a^2\sigma NM + b(N+M) + c}. \quad (25)$$

On the horizontal axis  $\beta_{12} = 0$ , eq.s (24) and (25) require

$$\beta_{11}/18 = \exp(-a^2\sigma), \quad (26)$$

in the leading order of  $NM$ .

Then, considering the area law off the horizontal axis, we have

$$\beta_{12}/18 = C \exp(-2a^2\sigma), \quad (27)$$

in the same order. Thus parabolic relation,  $\beta_{12} \propto \beta_{11}^2$ , follows.

In a differential form, we have

$$\frac{d\vec{\beta}}{da^2} = -\sigma \begin{pmatrix} 1 & 0 \\ 0 & 2 \end{pmatrix} \vec{\beta}. \quad (28)$$

Now, we will assemble the two models into an equation. It is conveniently expressed by means of dimensionless variable  $s = a\sqrt{\sigma}$  as

$$\frac{d\vec{\beta}}{ds} = -2s \begin{pmatrix} 1 + \frac{\zeta_1}{s} & 0 \\ 0 & 2 + \frac{\zeta_2}{s} \end{pmatrix} \vec{\beta} + \frac{1}{s} [\mathbf{A}\vec{\beta} - B(\beta_n) \frac{\vec{n}}{|\vec{n}|^2}] \quad (29)$$

Here, we keep next order in  $a$  in the nonperturbative term as free parameters,  $\zeta_1$  and  $\zeta_2$ . The equation (29) reduces to the eq.(16) at small  $a$  and the eq.(28) at large  $a$ . [25]

## 5.1 Global feature of the flow by the model

We will apply the model flow equation (29) to the flow data obtained in the section 3. The two vectors  $\vec{v}$  and  $\vec{w}$  are parametrized as  $\vec{v} = (\cos \theta', \sin \theta')$  and  $\vec{w} = (\cos \theta, \sin \theta)$ . Then the matrix  $\mathbf{A}$  with a zero and a finite eigen-value  $\lambda$  is given by

$$\mathbf{A} = \frac{\lambda}{(\vec{v} \cdot \vec{w}_T)} \vec{v} \otimes \vec{w}_T^t = \frac{\lambda}{\sin(\theta - \theta')} \begin{pmatrix} \sin \theta \cos \theta' & -\cos \theta \cos \theta' \\ \sin \theta \sin \theta' & -\cos \theta \sin \theta' \end{pmatrix}, \quad (30)$$

where  $\vec{w}_T$  is a vector orthogonal to  $\vec{w}$ . The vector  $\vec{n}$  is given by  $\vec{n} = (1, \cot(-\theta'))$ .

In the first, we describe global feature of the MCRG flow by the model. As discussed above, the vector  $\vec{w}$  specifies slant of the attractive line while the vector  $\vec{v}$  is a direction for approaching to it. The latter is matched with the flow data from plaquette action at  $\beta_{11} > 6$ . The eigenvalue  $\lambda$  is adjusted to reproduce the strength of coupling shift. Finally parameter  $\zeta$ 's are used to adjust the attraction towards the origin. Actually trajectories are not sensitive on  $\zeta$ 's.

Now we will see the behavior of a solution of the model flow equation (29). Initial conditions for  $\beta$ 's and  $a\sqrt{\sigma}$  are given by the data of plaquette action in table 4. [18, 21, 26] The parameters are taken so as to match the recently reported data of  $a\sqrt{\sigma}$  for Iwasaki action.[26]

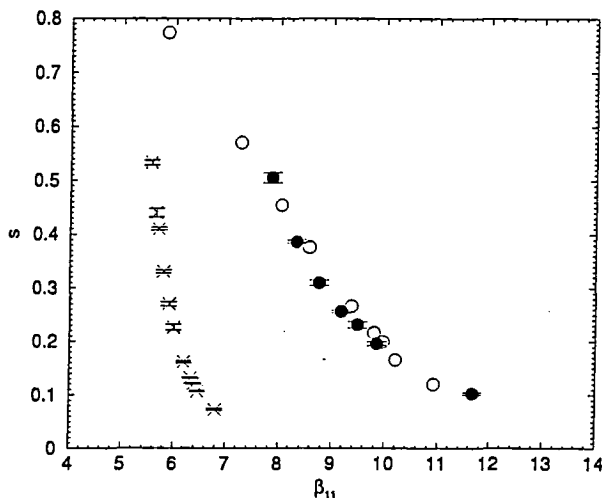


Figure 5: Flow trajectories by the model flow equation (29). The crosses are input data at plaquette action in the Table 4. Filled circles are the data of Iwasaki action [26]. Open circles are the calculated results by eq.(29).  $s$  stands for  $a\sqrt{\sigma}$ .

Fig.5 shows results of the model for

$$\theta = -0.156, \quad \theta' = -0.205, \quad \lambda = -0.5, \quad \zeta_1 = 0.1 \quad \zeta_2 = 0.0. \quad (31)$$

In spite of simplicity of the model, it reasonably connects the  $a\sqrt{\sigma}$  of the two different actions.

We will see output of the flow of the model in this parameter set. Fig.6 shows typical pattern of flows by the model. Points corresponding to the factor-2 blocking are also indicated by symbols on the trajectories.

As shown in Fig.6, the model well describes characteristic features of MCRG flow. Rapid approaching to the attractive stream is driven by the irrelevant coupling. This is manifest for the trajectory for higher  $\beta_{11}$ . Successively flows converge almost to a single curve in the strong coupling region although subtle crossing between them are seen. In the present model, rapid approach to the attractor leads this convergence.

At intermediate lattice spacings, both the nonperturbative term and asymptotic scaling term drive the trajectories. Finally, in the strong coupling region, nonperturbative term dominates and parabolic behavior of the trajectories sets on.

For further examination of the model, contours of constant lattice spacing are calculated and shown in Fig.7. Again, initial conditions are given in Table 4. The symbols show the

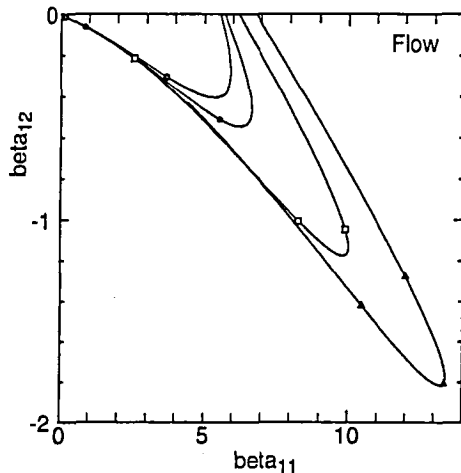


Figure 6: Flow trajectories by model

points with  $a\sqrt{\sigma} = 0.4099$ ,  $0.2702$  and  $0.1619$  while the data are those of  $aT_c = 4$  (open squares) and  $6$  (open circles). As seen in the figure, the contours of constant lattice spacing are consistently reproduced.

Another comparisons on the lattice spacing for tree Symanzik action and DBW2 action are made in Fig.7. As for the DBW2 action, scaling analysis has been also performed by Borici et al. [27] where  $\beta_{12}/\beta_{11} = -0.115$  instead of  $-0.1148$ . In Fig.8, lattice spacings for them are calculated by using initial values in Table 4. The flow model gives good description of the data for the tree Symanzik action, while systematic deviation at larger  $\beta_{11}$  for DBW2 action is seen. However the deviation seems not serious since flows are near turning points around DBW2 action and are strongly dependent on the parameters. Fine tuning will be beyond the role of the present simple model.

As a whole, we have found that the characteristics of the RG flow can be understood based on driving forces due to a marginal coupling, an irrelevant coupling term and a nonperturbative term corresponding to the area law.

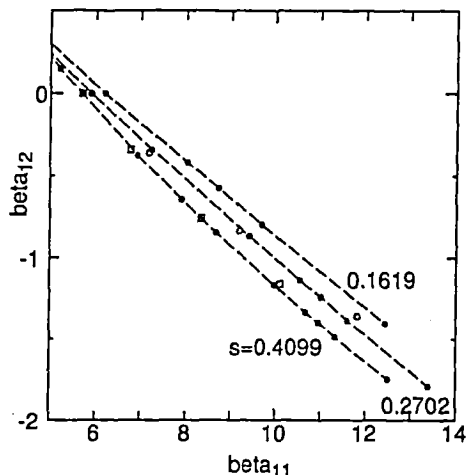


Figure 7: Contours of constant lattice spacing.  $s$  is  $a\sqrt{\sigma}$ . The data of  $aT_c = 4$  (open squares) and 6 (open circles) are also indicated.

| Initial values<br>( $\beta_{11}, \beta_{12}$ ) | $a\sqrt{\sigma}$                    | ref. | ( $\beta_{11}, \beta_{12}$ )<br>at $2a$ | ( $\beta_{11}, \beta_{12}$ )<br>at $4a$ |
|--|-------------------------------------|------|---|---|
| (5.55, 0.0)                                    | 0.5329(43)                          |      | (3.702, -0.3048)                        | (0.1319, -0.0143)                       |
| (5.65, 0.0)                                    | 0.4400(81)                          |      | (5.042, -0.4523)                        | (0.5741, -0.0423)                       |
| (5.70, 0.0)                                    | 0.4099(24)                          | [18] | (5.531, -0.5090)                        | (0.8626, -0.0629)                       |
| (5.80, 0.0)                                    | 0.3302(30)                          | [18] | (6.852, -0.6699)                        | (2.166, -0.1759)                        |
| (5.90, 0.0)                                    | 0.2702(37)                          | [18] | (7.898, -0.8008)                        | (3.805, -0.3577)                        |
| (6.00, 0.0)                                    | 0.2265(55)                          | [18] | (8.690, -0.8996)                        | (5.394, -0.5667)                        |
| (6.20, 0.0)                                    | 0.1619(19)                          | [18] | (9.902, -1.046)                         | (8.291, -1.006)                         |
| (6.338, 0.0)                                   | 0.132(1)                            | [21] | (10.51, -1.117)                         | (9.839, -1.255)                         |
| (6.40, 0.0)                                    | 0.1215(12)                          | [18] | (10.75, -1.143)                         | (10.42, -1.349)                         |
| (6.47, 0.0)                                    | $\sqrt{\sigma}/4.16(4)\text{GeV}^*$ | [26] | (11.10, -1.183)                         | (11.46, -1.521)                         |
| (6.80, 0.0)                                    | 0.0730(12)                          | [18] | (12.00, -0.1275)                        | (13.36, -0.1808)                        |

Table 4. Initial values of  $\beta_{11}$ ,  $\beta_{12}$  and lattice spacing  $a$ . The table includes calculated values of them at  $2a$  and  $4a$  by eq.(29). (\*:  $\sqrt{\sigma} = 420\text{MeV}$  is assumed.)

## 6 Discussion

In this work, the working space is limited to the two coupling space  $(\beta_{11}, \beta_{12})$ . As shown before, there is an evidence that the RT locates close to the plane. Although it is highly nontrivial fact, truncation effect which comes from the limitation of the coupling space should be examined. There are several indirect evidences that it may be important. As seen in Fig.1, shape of the attractor is less clear above  $\beta_{11} \sim 12$ . This suggests that the distance to the RT grows in this region. Another point is that the resultant couplings  $(\beta_{11}^V, \beta_{12}^V)$  by the Schwinger-Dyson equation after blocking gives larger lattice spacing (roughly 40-60 %) than twice of the original lattice spacing. One of possible reasons is the choice of minimal set of

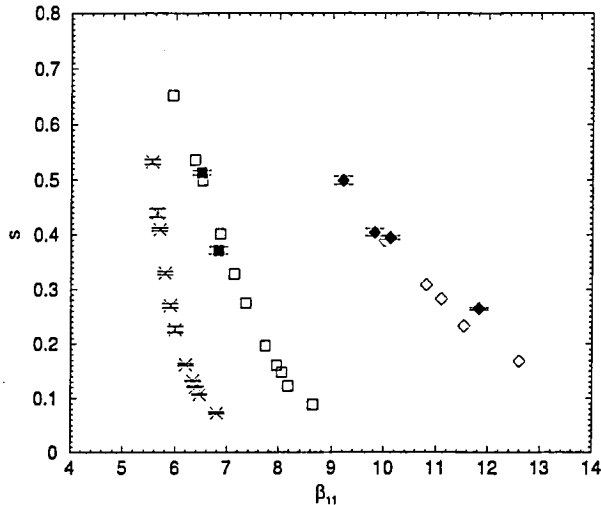


Figure 8: Lattice spacing versus  $\beta_{11}$ .  $s$  stands for  $a\sqrt{\sigma}$ . The cross is input data at plaquette action in the Table 4. Filled symbols are the data of tree Symanzik(square) and DBW2(diamond) actions. Corresponding open symbols are the predicted results by eq.(29).

loops in the Schwinger-Dyson equation. But the truncation effect may be another reason. See ref.([16]).

In order to clarify the situation, we perform a limited analysis in a three coupling space,  $(\beta_{11}, \beta_{12}, \beta_{twist})$  of which an action of twist loop is included,[24]

$$S = \beta_{twist} \sum_{n,\mu \neq \nu \neq \tau} [1 - \frac{1}{3} ReTr(P_{twist})]. \quad (32)$$

where

$$P_{twist}^{\mu\nu\tau} = U_{\mu}(n)U_{\nu}(n + \hat{\mu})U_{\tau}(n + \hat{\mu} + \hat{\nu})U_{-\nu}(n + \hat{\mu} + \hat{\nu} + \hat{\tau})U_{-\mu}(n + \hat{\mu} + \hat{\tau})U_{-\tau}(n + \hat{\tau}). \quad (33)$$

Blockings start from the points near the attractor in the two coupling spaces, i.e., the  $\beta_{twist} = 0$  sector. Results are shown in Fig.9. As shown in the figure, no sizable value of  $\beta_{twist}$  is generated on the points on the attractor. On the other hand, if we start from the points  $\beta_{11} \sim 10, \beta_{12} \sim -1.0$ , negative  $\beta_{twist}$  is induced as shown in Fig.9. This indicates that attractor in the three coupling space sits little below the  $\beta_{12} = 0$  sector in this region. Although more extensive studies are necessary to clarify the exact situation, it turned out that the attractor in two coupling space gives a good start point of improved actions.

## 7 Summary

We investigate the renormalization group (RG) flow of SU(3) lattice gauge theory in two coupling space,  $(\beta_{11}, \beta_{12})$ . An extensive numerical calculation of the RG flow of the lattice is made. Swendsen's blocking followed by effective action search using Schwinger-Dyson method is adopted to find renormalization effects. Analyses in the fourth quadrant in the coupling space reveals presence of an attractive stream. Trajectories are firstly attracted toward it and after that they move to origin along it. Stream converges to a curve in the strong coupling

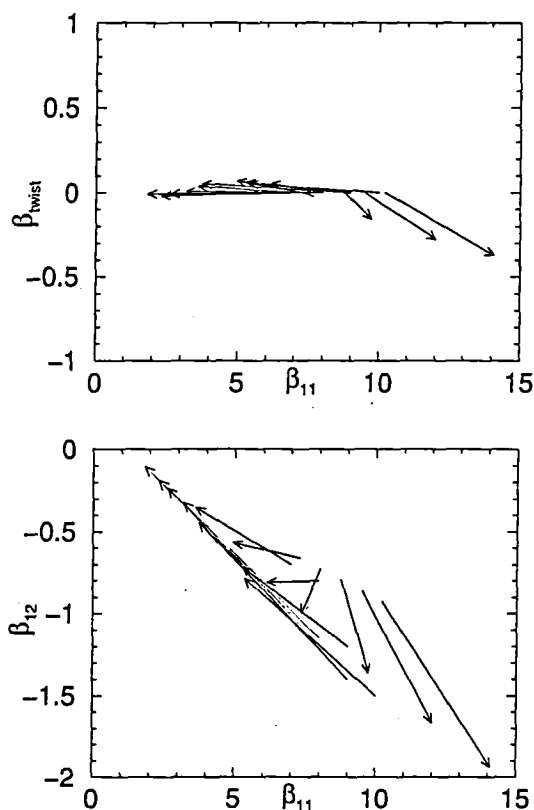


Figure 9: RG flow of SU(3) lattice gauge theory in three coupling space ( $\beta_{11}, \beta_{12}, \beta_{twist}$ ).

region. These features indicate that the RT locates close to the two coupling space and the attractive stream traces the RT. A model flow equation which consists of asymptotic scaling, an irrelevant coupling and a nonperturbative force corresponding to area law can reproduce the observed features. Scaling property of the action near the attractive stream is examined. It shows excellent restoration of rotational invariance. Effect of truncation is partly examined and it is found that renormalization effect to the outside of the two coupling space is small and attractive stream in the two coupling space gives a good start point of improvement.

## 8 Acknowledgments

All simulations have been done on CRAY J90 at Information Processing Center, Hiroshima University, SX-4 at RCNP, Osaka university and on VPP500 at KEK (National Laboratory for High Energy Physics). The authors would like to acknowledge M.Okawa for discussions on Schwinger-Dyson method. H.Matsufuru would like to thank the Japan Society for the Promotion of Science for financial support. This work is supported by the Grant-in-Aide for Scientific Research by Monbusho, Japan (No. ???? and No. ???).

## References

- [1] K.G. Wilson, in *Recent Developments in Gauge theories*, ed. G. t'Hooft (Plenum Press, New York, 1980) p.363.

- [2] R. Gupta, The Renormalization Group and lattice QCD", *From Actions to Answers*, ed. T. DeGrand and D. Toussaint, World Scientific 1990; Scaling, the Renormalization Group and Improved Lattice Actions", *Quantum Fields on the Computer*, Ed. M. Creutz, World Scientific, 1992.
- [3] QCD-TARO Collaboration, Phys.Rev.Letters,(1993) 71, 3963.
- [4] A. Gonzalez-Arroyo and M. Okawa, Phys.Rev.D 35 (1987) 672; Phys.Rev.B 35 (1987) 2108.
- [5] M. Hasenbusch, K. Pinn and C. Wierzkowski, Phys. Lett. B338 (1994) 308.
- [6] T. Takaishi, Mod. Phys. Lett. A10 (1995) 503.
- [7] A.Patel and R.Gupta, Phys.Lett. B 183 (1987) 193.
- [8] Y.Iwasaki, University of Tsukuba preprint, UTHEP-118, 1983.
- [9] P. Hasenfratz, F. Niedermayer, Nucl.Phys.B414(1994)785
- [10] QCD-TARO Collaboration, Nucl.Phys.B(Proc.Suppl.) 53 (1997) 938.
- [11] R.H. Swendsen, Phys.Rev.Lett. 42 (1979) 859.
- [12] M.Creutz, Phys.Rev.Lett. 50 (1983) 1441 ; M.Hasenbush, K.Pinn, and C.Wierzkowski, Phys.Lett. B 338 (1994) 308.
- [13] M. Creutz, Quarks, gluons and lattices", Cambridge Univ Press, 1985, Chapter 10.
- [14] K.Symanzik, Nucl.Phys.B 226 (1983) 187,205.
- [15] S. Itoh, Y. Iwasaki and T. Yoshie, Phys.Rev.D 33 (1986) 1806.
- [16] T. Takaishi, Phys. Rev. D 54 (1996) 1050.
- [17] I.R. McDonald and K. Singer, Discuss. Faraday, Soc. 43 (1967) 40.; A.M. Ferrenberg and R.H. Swendsen, Phys.Rev.Lett.61 (1988)2635.;63(1989)1195.
- [18] G.S. Bali and K. Schilling, Phys.Rev.D 46(1992) 2636.
- [19] Y. Iwasaki and K. Kanaya, K. Kaneko, T.Yoshié, Phys. Rev. D 56 (1997) 151.
- [20] B. Beinlich, F. Karsch, E. Laermann and A. Peikert, Eur. Phys. J. C6 (1999) 133-140
- [21] G. Boyd, J. Engels, F. Karsch, E. Laermann, C. Legeland, M. Lütgemeier and B. Petersson, Nucl.Phys.B 469 (1996) 419.
- [22] F. Karsch with B. Beinlich, J. Engels, R. Joswig, E. Laermann, A. Peikert and B. Petersson, Nucl.Phys.B (Proc.Suppl.) 53 (1997) 413.
- [23] Ph. de Forcrand et al., QCDTARO-collaboration , Nucl.Phys. B(Proc.Suppl.)63A-C (1998) 928-930.
- [24] Ph. deForcrand et al., QCDTARO-collaboration , Proceedings of the LATTICE98, Colorado,1998, Nucl.Phys. B(Proc.Suppl.)73 (1998) 924.

- [25] Ph. deForcrand et al., QCDTARO-collaboration , Proceedings of the LATTICE9p, Pisa,1999,
- [26] Equation of state for pure SU(3) gauge theory with renormalization group improved action  
M. Okamoto et al., UTHEP-402, hep-lat/9905005, (1999)
- [27] A.Borici and R.Rosenfelder, Nucl. Phys. B(Proc.Suppl.)63A-C (1998) 925.